Optica Applicata, Vol. XXXIX, No. 3, 2009

Genetic algorithm for band gap optimization under light line in two-dimensional photonic crystal slab

WEI JIA*, LIYONG JIANG, HIPENG LI, GAIGE ZHENG, XIANGYIN LI

School of Sciences, Nanjing University of Science and Technology, Nanjing 210094, P.R. China

*Corresponding author: njustjw@yahoo.com.cn

An optimization algorithm is used to design a two-dimensional photonic crystal slab for large absolute band gaps under light line. In this procedure, the unit cell of the crystal is composed of a number of circular holes in silicon substrate arranged in hexagonal lattice. By optimizing the location and radius of circular hole in the unit cell, we present four designs considering different circular hole numbers. The genetic algorithm finally yielded a photonic crystal with an absolute common band gap of $0.0788(2\pi c/a)$ at the mid-frequency of $0.3714(2\pi c/a)$.

Keywords: two-dimensional photonic crystals, photonic band gap under light line, genetic algorithm.

1. Introduction

Since the initial prediction of YABLONOVITCH [1] and SAJEEV JOHN [2], photonic crystals (PCs) have attracted a great deal of interest as new optical materials due to their unique characteristics and potential applications in photonic and optical telecommunication devices. Analogous to the electronic band gaps in semiconductors, the PCs are characterized by photonic band gaps (PBGs), which provide the possibility to control photons in the same way as the control of electrons. And in terms of the dimensionality of stacks, the PCs can be classified into three categories: one--dimensional (1D), two-dimensional (2D), and three-dimensional (3D) PCs [2–5]. Photonic crystal slab (PCS) is a peculiar structure of PCs, because it is not a "2D" PC, despite the resemblance: the finite thickness in the vertical direction introduces qualitatively new behavior, such as optical mirrors, limiters, filters and switches. Since many of the above applications take advantage of the band gap imposed by the periodic structure to the propagating electromagnetic fields, it is mostly of interest to design a PCS with a maximum possible band gap. It is known that the band gap of PCs is controllable by the dielectric constant contrast of its constituent materials [6], the type of its lattice [7], the filling factor [8], and the pattern used for the unit cell [9].

With the rapid improvement of the speed of modern computers, one may hope that a fast computer could help to design a 2D PC with a maximal absolute band gap. As

a global maximum seeking algorithm, the genetic algorithm (GA) [10] has been successfully applied in the design of 2D structures with large absolute band gaps in previous works [11]. However, there are still some problems in these designs. For example, the unit cell of structures presented in literature is composed of a large number of pixels (square rods) [12, 13], which is too complicated to fabricate in practical applications. Furthermore, the optimized band gaps in theses works are between very high frequency bands, above the light line, which makes the crystal implementation impossible in practical areas that only need band gaps under light line [14, 15]. There has also been a recent work involving the design of large band gap under light line using the GA. Nevertheless, the authors have only considered the designs for TE polarization [16]. Different from previous works, in this paper, we focus on the design of 2D PCS with large common band gaps (overlapped band gaps for both TE and TM polarizations) under light line. From the reference [17], we have seen the pore structure of 2D PCS with hexagonal lattice to have larger common band gaps than other structures. Hence, we expect to obtain a 2D PCS with a very large absolute band gap by using a GA to optimize the geometrical parameters of each hole in the unit cell.

2. Optimization algorithm

The optimization process is defined for a 2D PCS with hexagonal lattice consisting of two different materials with refractive index $n_{\text{high}} = 3.4$ (Si) and $n_{\text{low}} = 1$ (air). We assume that the thickness of the PCS is $0.5a$ along the Z-axis, and their areas on both sides of PCS are air-infinite [18]. The unit cell dimensions of X-axis and Y-axis are shown in Fig. 1. The unit cell is composed of a number of circular holes in silicon substrate. Figure 1 depicts a sample configuration of three circular holes in silicon substrate in the unit cell. Gray color is used to represent high dielectric material and white color is used to represent air. The location and radius of the center of each hole are represented by $\sigma = (x, y, r)$ before the holes overlap or hit the boundaries of the unit cell. The photonic crystal bands were solved by plane-wave expansion method, which was implemented by a freely available software package. From the calculated bands, any band gap was obtained. We assume that the number of band gaps is l and

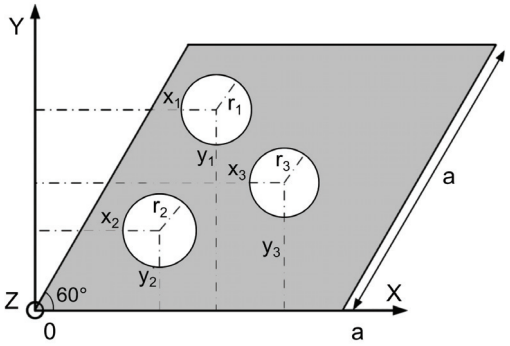

Fig. 1. The unit cell of a 2D PC with hexagonal lattice composed of three circular holes in silicon substrate.

each band gap can be defined as G_1, G_2, G_3, ..., G_l. To achieve large stop-bands, the objective function in this paper can be described as

$$F = \text{maximum}\left[G_1, G_2, G_3, \ldots, G_l\right] \tag{1}$$

A conventional binary GA is used here for the optimization of objective function. We begin the GA by randomly creating a population P_0 of N_c chromosomes (also called individuals) that are encoded by binary strings of a given length to represent possible schemes. For instance, the i-th chromosome can be expressed as the following sequence:

$$B_i = Bx_1 Bx_2 \ldots Bx_N By_1 By_2 \ldots By_N Br_1 Br_2 \ldots Br_N, \quad (i = 1, 2, \ldots, N_c) \tag{2}$$

where

$$Bx_j = C_1 C_2 \ldots C_P, \quad (j = 1, 2, \ldots, P) \tag{3}$$

$$By_j = K_1 K_2 \ldots K_Q, \quad (j = 1, 2, \ldots, Q) \tag{4}$$

$$Br_j = T_1 T_2 \ldots T_M, \quad (j = 1, 2, \ldots, M) \tag{5}$$

In the above formulation, Bx_j, By_j, and Br_j can represent the binary value of x, y, and r for the j-th hexagonal high dielectric cylinders, respectively. After encoding, the fitness value of each chromosome that decides its fraction surviving will be evaluated by the objective function.

Among GA's operation, we used three steps to propagate a new generation of chromosomes from the current generation:

Selection. The selection operator (also known as roulette-wheel selection) chooses two chromosomes randomly from the original population P_0 and keeps down the better one with higher fitness value to form a new population. This process is repeated until the new population P_s contains N_c chromosomes.

Crossover. The crossover operator randomly chooses a pair of parent chromosomes $B_{\text{parent, 1}}$ and $B_{\text{parent, 2}}$, which were mated to produce a child chromosome B_{child} by taking a random convex combination of the parent vectors. After crossover, another new population P_{sc} is created.

Mutation. After crossover, mutation operator is applied to prevent premature convergence. Mutation simply negates each bit in the population with a given probability p_m and then creates anew population P_{scm}. Then the chromosomes of P_{scm} are reevaluated, and the process begins anew with selection.

The algorithm is terminated when either a design goal is reached, or no process is observed in the population for several generations, which is usually represented by a maximum generation N_G. Finally, the best chromosome will be decoded to provide the optimization solution. Not that p_c and p_m are two important control parameters for GA. And it is necessary to choose suitable values of them for the sake of achieving as

high calculation efficiency and effectiveness as possible. Mass numerical experiments have checked that p_c in the range of 0.6–0.9 and p_m in the range of 0.001–0.1 are appropriate for most GA projects. In particular, we choose $p_c = 0.9$ and $p_m = 0.005$ in this paper according to many GA designers' recommendations. Moreover, considering both calculation precision and velocity, we set $N_c = 300$ and $N_G = 100$ for calculation.

3. Numerical results

In this section, we will present several optimization projects considering different number of circular holes in the unit cell. To improve the calculation velocity, in the searching process, 520 plane-waves are employed to analyze the band structures. In order to have high accuracy, the final structure after each optimization is analyzed further using 1300 plane-waves, as presented here.

The first optimization project assumes that the unit cell consists of one circular hole in silicon substrate. The dimension and the positions of the center of these circular holes are optimized in order to achieve a large higher-order stop-band. The obtained optimum structure and its band diagram are depicted in Fig. 2. This structure has an absolute band gap of $0.0706(2\pi c/a)$ at the mid-frequency of $0.3692(2\pi c/a)$. The relative bandwidth for this structure is 19.12%. The band gap of this structure occurs between the second and third TE bands and the first and second TM bands (Fig. 2). The radius and location of the center of each rod are represented by $\sigma_1 = (0.7495a, 0.4326a, 0.4323a)$.

In the second optimization project, it is assumed that the unit cell consists of two circular holes in silicon substrate. We obtain an optimum structure as shown in Fig. 3. The location of the center and radius of each circular hole are represented by $\sigma_1 = (1.0684a, 0.8096a, 0.0530a)$ and $\sigma_2 = (0.7495a, 0.4324a, 0.4323a)$, respectively.

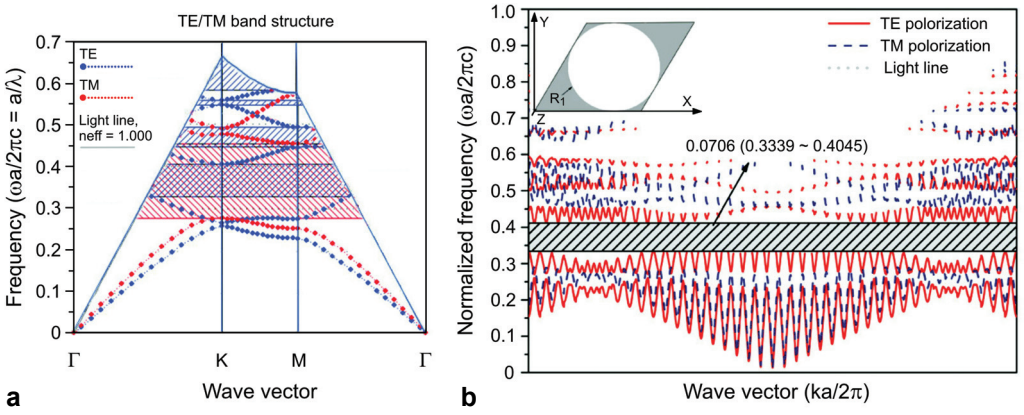

Fig. 2. The optimized structure with one circular hole in its unit cell and the corresponding band diagram for TM mode (solid lines) and TE mode (dotted lines); *Γ*, *K*, and *M* refer to the corner points of the 1/8 Brillouin zone – **a**. The optimized structure with one circular hole in its unit cell and the corresponding band diagram for TE and TM polarizations of full zone – **b**.

This structure has an absolute band gap of $0.0788(2\pi c/a)$ at the mid-frequency of $0.3714(2\pi c/a)$. The relative bandwidth of the absolute band gap is about 21.22%. The obtained optimum band gap of this structure is produced from the overlap of the TE gap between the second and third TE bands with TM gap between the first and second TM bands (Fig. 3).

The third optimization project is implemented assuming that the unit cell consists of three circular holes in silicon substrate. Figure 4 shows the optimized structure as well as its corresponding complete dispersion band diagram. The structure information

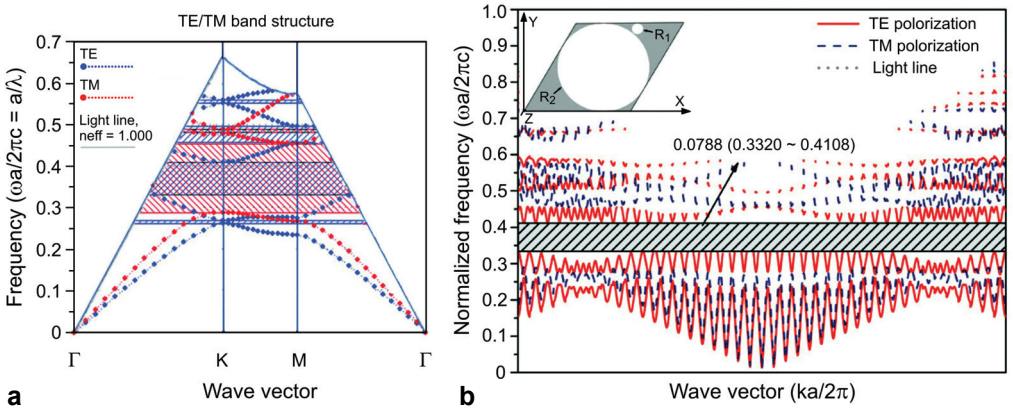

Fig. 3. The optimized structure with two circular holes in its unit cell and the corresponding band diagram for TM mode (solid lines) and TE mode (dotted lines); *Γ*, *K*, and *M* refer to the corner points of the 1/8 Brillouin zone – **a**. The optimized structure with two circular holes in its unit cell and the corresponding band diagram for TE and TM polarizations of full zone – **b**.

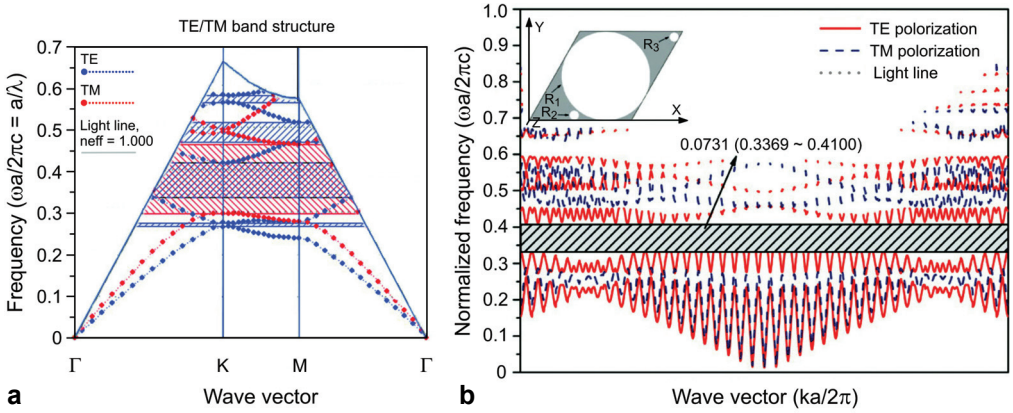

Fig. 4. The optimized structure with three circular holes in its unit cell and the corresponding band diagram for TM mode (solid lines) and TE mode (dotted lines); *Γ*, *K*, and *M* refer to the corner points of the 1/8 Brillouin zone – **a**. The optimized structure with three circular holes in its unit cell and the corresponding band diagram for TE and TM polarizations of full zone – **b**.

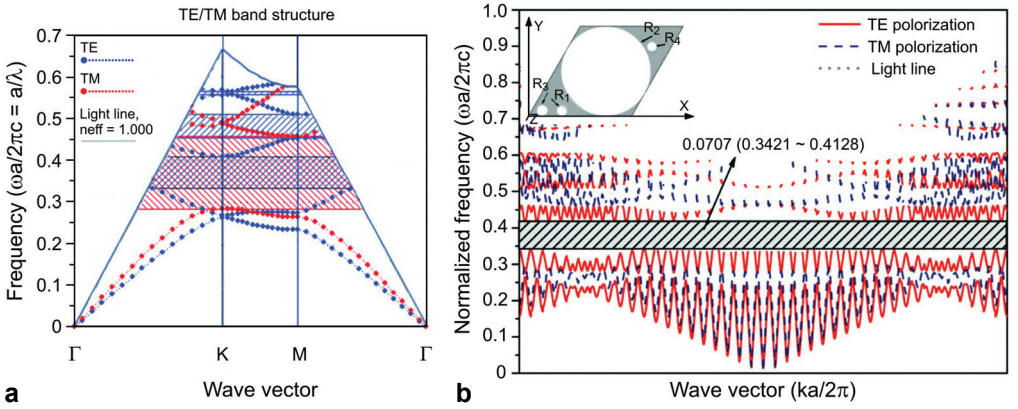

Fig. 5. The optimized structure with four circular holes in its unit cell and the corresponding band diagram for TM mode (solid lines) and TE mode (dotted lines); *Γ*, *K*, and *M* refer to the corner points of the 1/8 Brillouin zone – **a**. The optimized structure with four circular holes in its unit cell and the corresponding band diagram for TE and TM polarizations of full zone – **b**.

of each hole is represented by $\sigma_1 = (0.7506a, 0.4307a, 0.4320a)$, $\sigma_2 = (0.4415a, 0.0484a, 0.0433a)$, and $\sigma_3 = (1.4157a, 0.8089a, 0.0440a)$, respectively. Compared with the above design, this structure presents an absolute band gap of about $0.0731(2\pi c/a)$ at a lower mid-frequency of $0.3734(2\pi c/a)$. The common band gap of this structure still occurs between the second and third TE bands and first and second TM bands (Fig. 4). The ratio of the bandwidth to the mid-frequency of the band gap is about 19.57%.

The final run of the GA is implemented with the unit cell consisting of four circular holes in silicon substrate. This optimum structure and its corresponding band diagram are depicted in Fig. 5. In this case, the absolute bandwidth of the common band gap is further decreased to $0.0707(2\pi c/a)$, which is located at the mid-frequency of $0.3774(2\pi c/a)$ (the relative bandwidth for this structure is 18.73%). This stop-band is

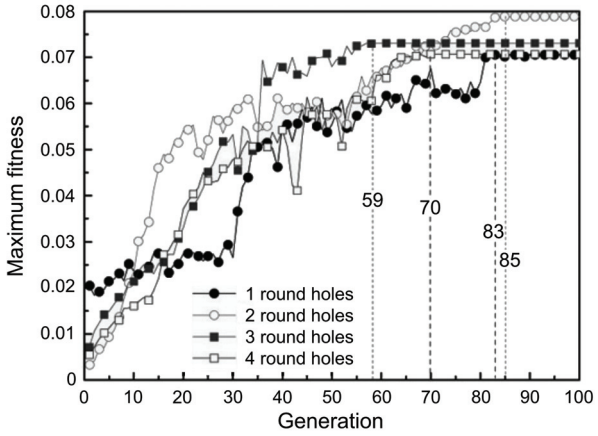

Fig. 6. Best fitness of the population as a function of generation.

also produced from the overlap of the TE gap between the second and third TE bands with TM gap between the first and second TM bands (Fig. 5). The geometrical parameters of each hole in the optimum unit cell (Fig. 5) are represented by σ_1 = = (0.3234a, 0.0500a, 0.0488a), σ_2 = (0.7504a, 0.4355a, 0.4305a), σ_3 = (0.1322a, 0.0531a, 0.0502a), and σ_4 = (1.6010a, 0.7302a, 0.0480a), respectively.

Statistic information of the evolutionary process can be described by Fig. 6, where the best fitness as a function of generation is shown for each optimization project. It can be found that the maximum fitness is improved over and over again when it remains unchanged over a number of successive generations. This performance is mainly due to the floating crossover and mutation probabilities in evolutionary process. From the plot, the optimized structures in each optimization project are obtained through 83, 85, 59 and 70 generations, respectively. To the best of our knowledge, the design of two circular holes in the unit cell found in this paper has the largest common band gap under light line among all the 2D dielectric PCSs of hexagonal lattices that have been reported in the literature. In addition, this optimum structure is composed of simple circular holes in silicon substrate which may be fabricated more easily in the desired wavelength range.

4. Conclusions

The ability of a modified genetic algorithm to find a novel photonic crystal slab with large absolute band gaps under light line is demonstrated. In this procedure, the geometrical parameters of the unit cell correspond to a chromosome consisting of a binary sequence. The crossover and mutation probabilities in evolutionary process can be adjusted adaptively according to the value of individual fitness and dispersion of degree of population. As numerical examples, four optimal photonic crystal structures with large band gaps under light line are obtained. The absolute bandwidths for these band gaps are 0.0706($2\pi c/a$), 0.0788($2\pi c/a$), 0.0731($2\pi c/a$), and 0.0707($2\pi c/a$), respectively. As demonstrated by this and previous works, genetic algorithms are an effective tool for the design of photonic structures with complex morphologies that have unique optical properties.

References

[1] YABLONOVITCH E., *Inhibited spontaneous emission in solid-state physics and electronics*, Physical Review Letters **58**(20), 1987, pp. 2059–2062.

[2] SAJEEV JOHN, *Strong localization of photons in certain disordered dielectric superlattices*, Physical Review Letters **58**(23), 1987, pp. 2486–2489.

[3] NODA S., TOMODA K., YAMAMOTO N., CHUTINAN A., *Full three-dimensional photonic bandgap crystals at near-infrared wavelengths*, Science **289**(5479), 2000, pp. 604–606.

[4] WINN J.N., FINK Y., FAN S., JOANNOPOULOS J.D., *Omnidirectional reflection from a one-dimensional photonic crystal*, Optics Letters **23**(20), 1998, pp. 1573–1575.

[5] LI Z.-Y., WANG J., GU B.-Y., *Creation of partial band gaps in anisotropic photonic-band-gap structures*, Physical Review B **58**(7), 1998, pp. 3721–3729.

[6] LI Z.-Y., GU B.-Y., YANG G.-Z., *Large absolute band gap in 2D anisotropic photonic crystals*, Physical Review Letters **81**(12), 1998, pp. 2574–2577.
[7] CASSAGNE D., JOUANIN C., BERTHO D., *Hexagonal photonic-band-gap structures*, Physical Review B **53**(11), 1996, pp. 7134–7142.
[8] LI Z.Y., LIN L.L., GU B.Y., YANG G.Z., *Photonic band gaps in anisotropic photonic crystals*, Physica B: Condensed Matter **279**(1), 2000, pp. 159–161.
[9] SUSA N., *Large absolute and polarization-independent photonic band gaps for various lattice structures and rod shapes*, Journal of Applied Physics **91**(6), 2002, pp. 3501–3510.
[10] GOH J., FUSHMAN I., ENGLUND D., VUKOVIC J., *Genetic optimization of photonic bandgap structures*, Optics Express **15**(13), 2007, pp. 8218–8230.
[11] ANDERSON C.M., GIAPIS K.P., *Symmetry reduction in group 4mm photonic crystals*, Physical Review B **56**(12), 1997, pp. 7313–7320.
[12] LINFANG SHEN, ZHUO YE, SAILING HE, *Design of two-dimensional photonic crystals with large absolute band gaps using a genetic algorithm*, Physical Review B **68**(3), 2003, p. 035109.
[13] LINFANG SHEN, SAILING HE, SANSHUI XIAO, *Large absolute band gaps in two-dimensional photonic crystals formed by large dielectric pixels*, Physical Review B **66**(16), 2002, p. 165315.
[14] ZAREI S., SHAHABADI M., *Achieving large higher-order stop-bands in two-dimensional photonic crystals using a real-valued genetic algorithm*, Journal of Optics A: Pure and Applied Optics **10**(8), 2008, p. 085203.
[15] GHATAN Z., FALLAHI A., MAKKI B., SHAHABADI M., LUCAS C., BAHRAMI F., *A novel 2D genetic algorithm for band gap optimization of two-dimensional photonic crystals*, 2006 IEEE Congress on Evolutionary Computation, CEC 2006, pp. 3231–3235.
[16] PREBLE S., LIPSON M., LIPSON H., *Two-dimensional photonic crystals designed by evolutionary algorithms*, Applied Physics Letters **86**(6), 2005, p. 061111.
[17] VILLENEUVE P.R., PICHE M., *Photonic band gaps in two-dimensional square and hexagonal lattices*, Physical Review B **46**(8), 1992, pp. 4969–4972.
[18] NOTOMI M., SHINYA A., MITSUGI S., KURAMOCHI E., RYU H.Y., *Waveguides, resonators and their coupled elements in photonic crystal slabs*, Optics Express **12**(8), 2004, pp. 1551–1561.

Received January 23, 2009
in revised form March 14, 2009